

# Random-walk approach to the two-component random-conductor mixture: Perturbing away from the perfect random resistor network and random superconducting-network limits

D. C. Hong,\* H. E. Stanley, and A. Coniglio†

Center for Polymer Studies and Department of Physics, Boston University, Boston, Massachusetts 02215

A. Bunde

Center for Polymer Studies and Department of Physics, Boston University, Boston, Massachusetts 02215  
and Fakultät für Physik, Universität Konstanz, 7750 Konstanz, West Germany

(Received 24 June 1985)

We develop a random-walk approach that permits one to study novel physical phenomena that occur in the random two-component mixture of good and poor conductors. Our work significantly generalizes the previous body of knowledge on the random resistor network (pure “ant” limit) in which the poor-conductor species has *infinite* resistance, and the random superconductor network (pure “termite” limit) in which the good-conductor species has *zero* resistance. We find that for any fixed value of the concentration  $p$  of good conductors, we can map a system that is nearer the ant limit to one that is nearer the termite limit. Specifically, we find  $R^2(1, h, t/h) = R^2(h^{-1}, 1, t)$  where  $R^2(\sigma_a, \sigma_b, t)$  is the mean-square displacement of the walker, and  $h = \sigma_b/\sigma_a$  is the ratio of the conductivity of the poor and good components. This exact transformation permits one to develop a scaling theory for the general two-component case, which reduces to the known results for the ant limit and predicts dramatically new behavior for the termite limit. We test the scaling predictions extensively by Monte Carlo simulation methods. Finally, we develop an analogy with a simple magnetic system, in which the role of the magnetic field is played by the conductivity ratio  $h$ .

## I. INTRODUCTION

How are the fundamental laws of diffusion and transport modified when the medium in question is a random  $AB$  mixture of good and poor conducting regions [Fig. 1(a)]? This question has received a considerable degree of recent attention for two limiting cases:<sup>1-7</sup> (i) The random resistor network (RRN), or pure “ant” limit, for which  $B$ , the poor-conducting species, has zero conductance,<sup>1,8-12</sup> and (ii) The random superconducting network (RSN), or pure “termite” limit,<sup>2-7</sup> for which  $A$ , the good-conducting species, has infinite conductance.

The terms ant and termite arise from the fact that one can replace the conductivity problem with a diffusion problem using the Nernst-Einstein relation.<sup>13</sup> For the RRN limit, no diffusion can occur on the component with

zero conductance, so the constrained diffusion problem is rather like an “ant in a labyrinth.”<sup>1</sup> For the RSN limit, the diffusion can occur everywhere since both components conduct, but the fact that the good conductor species has zero resistance means that the diffusion is remarkably different in this region than elsewhere. Some years ago de Gennes invented the term “termite diffusion” to describe this subtle phenomenon.<sup>2</sup> However, to date there has been no clear statement of exactly how to properly define or measure this phenomenon,<sup>2-5</sup> in contrast to the ant limit where the diffusion is simply constrained to one component.<sup>2-5</sup> There are many reasons for the current upsurge of interest in this problem.

(i) One reason is that there are many experimental systems that are random and inhomogeneous.<sup>7</sup> For example, a rock is composed of tiny grains of different conductivities (to heat, to fluid flow, to electricity, etc.). To the extent that such inhomogeneous materials are also random, we may think of using a site-random description of this material “lattice-gas” description. One first coarse grains the material and then assigns to each cell one of two conductivities  $\sigma_a$  and  $\sigma_b$ . Calculations based upon such a straightforward approach have been usefully compared with a wide range of experiments,<sup>6,7,14-20</sup> from conductivities of thin films of lead depositions on an insulating substrate<sup>7</sup> (roughly the RRN limit) to thin films of superconducting material vacuum deposited on a normal substrate<sup>6</sup> (roughly the RSN limit). Moreover, ionic conductors mixed with a dispersed insulating phase represent random heterogeneous materials, where both limits seem to play an important role.<sup>14</sup>

(ii) A second reason is related, perhaps, to the reason

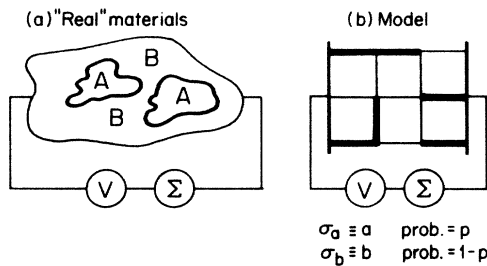


FIG. 1. (a) Schematic illustration of a random two-component composite material before coarse graining. (b) Replacement by equivalent random network with two conductances  $a = \sigma_a$  (probability  $p$ ) and  $b = \sigma_b$  (probability  $1-p$ ).

why the Ising model has always been of great interest: It is an extremely simple model that captures the essential physics of a realistic system in nature. The analog of the Ising model for random inhomogeneous materials is a mixture of sites (or bonds) randomly distributed on a lattice—see, e.g., Fig. 1(b). The sites (or bonds) are assumed for simplicity to have only two possible values of the conductance,

$$\begin{aligned} \sigma_a & \text{ (probability } p \text{) ,} \\ \sigma_b & \text{ (probability } 1-p \text{) .} \end{aligned} \quad (1.1)$$

By convention, we choose  $\sigma_a > \sigma_b$ , so that the ratio  $h = \sigma_b / \sigma_a$  is always less than unity.

Conventionally, one wants to know the *macroscopic* magnetization of an Ising ferromagnet composed of elements (spins) whose *microscopic* property is a two-valued variable. Similarly, we *now* want to know the *macroscopic* conductivity which depends on all possible configurations of the *microscopic* elements (conductors) whose property is again a two-valued quantity ( $\sigma_a$  and  $\sigma_b$ ).

The two limiting cases mentioned above can now be discussed more precisely (Fig. 2): (a) In the RRN limit, the large conductance is set to unity and the small conductance is set to zero. As the percolation threshold  $p_c$  is approached from above, the macroscopic conductivity  $\Sigma$  approaches zero with a critical exponent  $\mu$ ,<sup>7,21</sup>

$$\Sigma \sim (p - p_c)^\mu . \quad (1.2a)$$

(b) In the RSN limit, the small conductance is set to unity, and the large conductance is infinite. As the percolation threshold is approached from below, the conductivity diverges to infinity with an exponent  $s$ .<sup>6,22,23</sup>

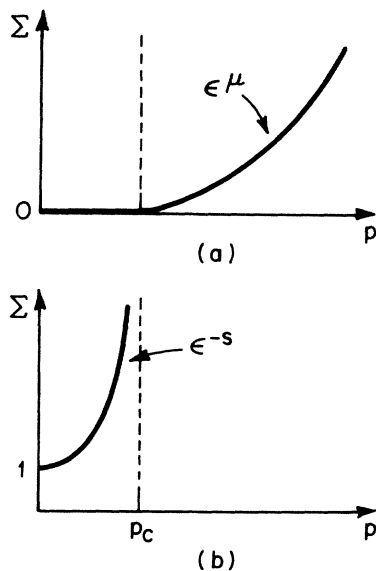


FIG. 2. Schematic dependence on  $p$  of the macroscopic conductivity  $\Sigma$  for two limiting cases of the present model: (a) the random resistor network (RRN) or ant limit, and (b) the random superconductor network (RSN) or termite limit. The corresponding exponents  $\mu$  and  $s$  are equal for  $d=2$ .

$$\Sigma \sim (p_c - p)^{-s} . \quad (1.2b)$$

The traditional approach to the RRN limit has been to replace Kirchhoff's laws by an equivalent diffusion problem, where the macroscopic conductivity is related to the diffusion constant  $D$  by the Nernst-Einstein relation,

$$\Sigma \sim nD , \quad (1.3)$$

where  $n$  is the density of the charge carriers.<sup>24</sup>

## II. RANDOM-WALK MODEL FOR THE CONDUCTIVITY OF A TWO-COMPONENT RANDOM MIXTURE

In this section, we briefly explain the model we have been developing to describe—using random walks—the conductivity of a general two-component random mixture.<sup>3,5</sup> Perhaps the best starting point is the pure ant limit in which the conductance of the poor conducting species tends to zero ( $\sigma_b = 0$ ). In this case, the Nernst-Einstein theorem applied to this case tells us that the macroscopic conductivity  $\Sigma$  (measured, e.g., by a pair of bus bars—see Fig. 1) is proportional to the diffusion constant  $D$ .

It is convenient to imagine a randomly diffusing particle which jumps from site to site over potential barriers. Each barrier has the same height if the bond has conductance  $\sigma_a$ , while the barrier is infinite in height if the bond has conductance  $\sigma_b$  (see Fig. 3). Thus, when the particle is at a boundary between two bonds with conductivities  $\sigma_a = 1$  and  $\sigma_b = 0$ , it will be “reflected” with probability unity by the zero conductivity bond. We could say that its jump frequency into the high-conductivity region is  $f_a = 1$ , while its jump frequency into the low-conductivity region is  $f_b = 0$ . Similar remarks apply to the termite or RSN limit, except that now  $f_a \rightarrow \infty$  and  $f_b = 1$ . For the case of a *general inhomogeneous material*,  $f_a$  and  $f_b$  are both finite constants, different from zero or infinity. The ratio  $h = f_b / f_a$  is zero for both the RRN and RSN limits, but for the general inhomogeneous material  $h$  is a number between zero and one. Note that since  $f_a \sim \sigma_a$  and  $f_b \sim \sigma_b$ ,  $h$  is also given by

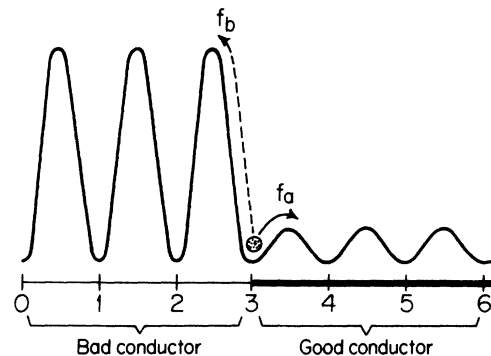


FIG. 3. Schematic illustration of our random-walk model for a one-dimensional lattice, showing the presence of a boundary between a good-conductor cluster of conductors  $\sigma_a$  and a poor-conductor cluster of conductors  $\sigma_b$ . The corresponding jump frequencies  $f_a$  and  $f_b$  determine, through Eq. (2.2), the probability of a particle being reflected at the boundary.

$$h = \sigma_b / \sigma_a = f_b / f_a. \quad (2.1)$$

With the foregoing picture in mind, we can now state clearly the random-walk model of a general two-component inhomogeneous material. Place a walker on a  $d$ -dimensional lattice made of two kinds of bonds,  $A$  and  $B$  (for illustration,  $d=1$ ; the general- $d$  case is discussed in Appendix B). The walker carries two coins, weighted and unweighted, and a clock. Without loss of generality, let the origin be well inside a high-conductivity  $A$  region. At each tick of the clock, the walker tosses the unweighted coin and moves to the left or right depending on the outcome of the coin toss. When the walker comes to a site on the boundary between the  $A$  region and the  $B$  region, it tosses the other coin that is weighted with probability

$$P_a = f_a / (f_a + f_b) = 1 / (1 + h), \quad (2.2a)$$

to stay in the  $A$  region, and a probability

$$P_b = f_b / (f_a + f_b) = h / (1 + h), \quad (2.2b)$$

to go outside into the  $B$  region. In the event that the walker steps outside the  $A$  region, then he must slow down by the ratio  $f_a / f_b$ . For example, if the conductivity of the  $B$  region is ten times smaller than that of the  $A$  region, then  $f_b$  is ten times smaller than  $f_a$  ( $h=0.1$ ) and the walker steps *only* after every ten ticks of its clock.

Limiting cases of our random walk model are as follows: (i)  $h=1$ . There is no distinction between regions, no reflection on the boundaries ( $P_a = P_b$ ), and no difference in walk speed on and off the  $A$  clusters. (ii)  $h \ll 1$ . The walker now moves at one step per clock tick when it is on an  $A$  cluster, and is almost always reflected when it comes to the boundary. Extremely rarely it passes out of an  $A$  region and into a  $B$  region, whereupon it walks much, much slower—taking a new step only after its clock has made  $h^{-1}$  ticks. Statistically speaking, in a very large time  $\gg h^{-1}$ , the walker performs  $O(f_a)$  moves in the  $A$  region and  $O(f_b)$  moves in the  $B$  region. Suppose we make a motion picture of the walker's motion. Then we see that the walker is reflected from the walls almost all of the time, and only very rarely—roughly once per  $h^{-1}$  trials—will come outside the cluster (see Appendix B). When this does occur, its motion will slow down by a factor of  $h$ . Let us now speed up the motion picture projector by a factor of  $1/h$  so that the walker is now taking *one* step per unit of time while in the  $B$  region. Then, when it finally encounters an  $A$  cluster, it moves onto it with a high probability,  $1/(1+h)$ , and proceeds to move about the  $A$  cluster with a motion that is *also sped up by the same factor*  $1/h$ . Thus the original ant who stepped normally on an  $A$  cluster and *extremely slowly* on  $B$  clusters has suddenly been transformed into a termite who moves normally on  $B$  clusters and *extremely fast* on  $A$  clusters. Indeed, the only difference between the two domains, ant (RRN domain) and termite (RSN domain), is the *definition* of the time scale. We shall see that this simple observation can be formalized in terms of a rigorous transformation (Sec. III) and that the transformation in turn forms the basis of the scaling laws for the

ant and termite limits of the general two-component random mixture (see Sec. IV).

### III. GENERAL RESULTS (EXACT)

In this section we develop some quite general and rather surprising exact relations. These concern (a) the dc ( $\omega=0$ ) conductivity  $\Sigma$ , (b) the rms displacement  $R(t)$ , and (c) the ac conductivity  $\Sigma(\omega)$ . These relations lead to surprising consequences. For example, they show that physical laws in the vicinity of the RSN limit are *identical* to those in the vicinity of the RRN limit. Since the relations hold for any fixed  $p$ , we have suppressed the  $p$  dependence in this section.

#### A. Proof that $\Sigma(h^{-1}, 1) = h^{-1} \Sigma(1, h)$

The content of this relation, treated previously by Efros and Shklovskii<sup>22</sup> and by Straley,<sup>25</sup> is indicated schematically in Fig. 4(a). It follows from the homogeneity relation

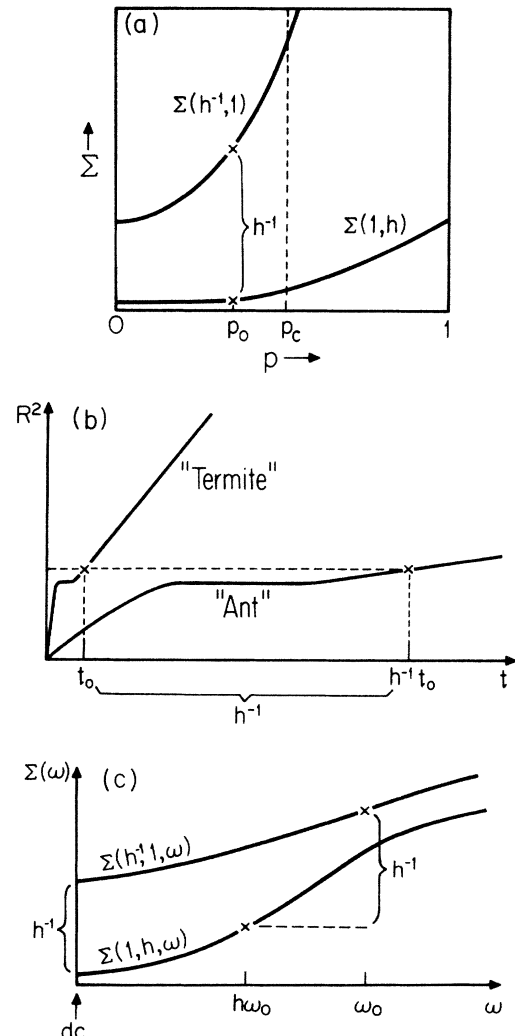


FIG. 4. Illustration of the exact relation derived in Sec. III for (a)  $\Sigma$ , (b)  $R^2$ , and (c)  $\Sigma(\omega)$ . The curly bracket means to multiply by the transformation factor  $h^{-1}$ .

$$\Sigma(\lambda\sigma_a, \lambda\sigma_b) = \lambda\Sigma(\sigma_a, \sigma_b), \quad (3.1)$$

which is a functional equation holding for all positive values of  $\lambda$ . If we set  $\lambda = 1/\sigma_a$ , then

$$\sigma_a \Sigma(1, \sigma_b/\sigma_a) = \Sigma(\sigma_a, \sigma_b). \quad (3.2a)$$

Alternatively, we can set  $\lambda = 1/\sigma_b$ ,

$$\sigma_b \Sigma(\sigma_a/\sigma_b, 1) = \Sigma(\sigma_a, \sigma_b). \quad (3.2b)$$

Combining (2.2a) and (2.2b), we have

$$\Sigma(h^{-1}, 1) = h^{-1}\Sigma(1, h), \quad (3.3)$$

where  $h = \sigma_b/\sigma_a$  as before. This result holds for *all* values of  $h$ . In the limit  $h \rightarrow 0$ , the left-hand side approaches  $\Sigma_T = \Sigma(\infty, 1)$  and the right-hand side approaches  $h^{-1}\Sigma_A = h^{-1}\Sigma(1, 0)$ . Note the following corollary: Since the Nernst-Einstein relation must hold for the two-component network, we can replace the conductivity by the diffusion constant in (3.3) and write

$$D(h^{-1}, 1) = h^{-1}D(1, h). \quad (3.4)$$

#### B. Proof that $R(h^{-1}, 1, t) = R(1, h, t/h)$

The above results can be generalized to the somewhat more microscopic function  $R(t) = (\langle r^2 \rangle)^{1/2}$ , the rms (averaged over all configurations) displacement of a random walker who moves on the general two-component system according to the rules described in Sec. II. This motion is thus characterized by two jump frequencies  $f_a \sim \sigma_a$  and  $f_b \sim \sigma_b$ , with  $h = f_b/f_a$ . If we consider now a second system in which, e.g., all jump frequencies were *doubled*, then the rms displacement of the original system would be reached in *half* the time. Note that since the jump frequency to the nearest neighbors only depends on the jumping ratio  $f_b/f_a$ , the path of the walker in the old and in the rescaled system are exactly the same. Thus an analogous statement holds for any transformation, and  $R$  must obey the functional equation

$$R(\lambda f_a, \lambda f_b, \lambda^{-1} t') = R(f_a, f_b, t'). \quad (3.5)$$

If we set  $\lambda = 1/f_a$ , then

$$R(1, f_b/f_a, t' f_a) = R(f_a, f_b, t'), \quad (3.6a)$$

while if  $\lambda = 1/f_b$ , we have

$$R(f_a/f_b, 1, t' f_b) = R(f_a, f_b, t'). \quad (3.6b)$$

Combining (3.6a) and (3.6b), we have a new result valid for any  $t$  and any  $h$ ,

$$R(h^{-1}, 1, t) = R(1, h, t/h), \quad (3.7)$$

where we have defined  $t = f_b t'$  so that

$$t' f_a = (t' f_b)(f_a/f_b) = t/h.$$

Thus the detailed behavior of the walker near the RSN limit differs from the behavior near the RRN limit by a simple change of time scale [Fig. 4(b)].

#### C. Proof that $\Sigma(h^{-1}, 1, \omega) = h^{-1}\Sigma(1, h, h\omega)$

Clearly this result reduces to (3.3) when  $\omega = 0$ . One first must establish the homogeneity relation

$$\Sigma(\lambda\sigma_a, \lambda\sigma_b, \lambda\omega') = \lambda\Sigma(\sigma_a, \sigma_b, \omega'), \quad (3.8)$$

which follows directly from the definition (1.3) and the homogeneity relation (3.5). Next we set  $\lambda = 1/\sigma_a$  to obtain the analog of (3.6a) and then we set  $\lambda = 1/\sigma_b$ . Equating these, we find

$$\Sigma(h^{-1}, 1, \omega) = h^{-1}\Sigma(1, h, h\omega), \quad (3.9)$$

where we have defined  $\omega = \omega'/\sigma_b$  so that

$$\omega'/\sigma_a = (\omega'/\sigma_b)(\sigma_b/\sigma_a) = \omega h.$$

Thus we can determine the conductivity at a frequency  $\omega_0$  in the *termite* regime if we know the conductivity in the *ant* regime at a frequency  $h\omega_0$  [Fig. 4(c)].

### IV. SCALING FOR THE CONDUCTIVITY OF A RANDOM MIXTURE

#### A. Conductivity scaling of $\Sigma(1, h, \epsilon)$ and the RRN limit

An analogy between the conductivity near the percolation threshold and the magnetization near the critical point was proposed by Straley.<sup>25</sup> For a ferromagnetic material, as  $\epsilon = (T - T_c)/T_c \rightarrow 0^-$ , one finds that the magnetization approaches zero as

$$M(\epsilon) \sim |\epsilon|^\beta. \quad (4.1a)$$

Similarly, for the pure RRN limit ( $h = 0$ ), we find as  $\epsilon = (p_c - p)/p_c \rightarrow 0^-$ , the dc conductivity *also* approaches zero,

$$\Sigma(1, h = 0, \epsilon) \sim |\epsilon|^\mu. \quad (4.1b)$$

This trivial analogy between  $M(\epsilon)$  and  $\Sigma(\epsilon)$  can be extended to the field variable  $h$ . (See Figs. 5 and 6.) For the ferromagnet at  $T = T_c$ ,

$$M(\epsilon = 0, h) \sim h^{1/\delta}, \quad (4.2a)$$

while for our problem  $h = \sigma_b/\sigma_a$  and

$$\Sigma(1, h, \epsilon = 0) \sim h^u, \quad (4.2b)$$

where  $u = \frac{1}{2}$  for  $d = 2$ .<sup>25</sup>

Next we obtain the functional form in the full  $\epsilon$ - $h$  plane near the origin  $\epsilon = h = 0$ . For the ferromagnet, the scaling *ansatz* states that asymptotically

$$M(\epsilon, h) \sim h^{1/\delta} g(\epsilon/h^\phi). \quad (4.3a)$$

Here  $\phi = 1/\beta\delta$  is the crossover exponent between  $\epsilon$  and  $h$ , while  $g(x)$  is the scaling function. Hence the natural scaling *ansatz* for the two-component random mixture is

$$\Sigma(1, h, \epsilon) \sim h^u g(\epsilon/h^\phi). \quad (4.3b)$$

Here

$$\phi = u/\mu \quad (4.4)$$

is the crossover exponent between  $\epsilon$  and  $h$ , and  $g(x)$  is the scaling function.

### B. Conductivity scaling for $\Sigma(h^{-1}, 1, \epsilon)$ and the RSN limit

The analogs of (4.1) and (4.2) for the RSN limit are

$$\Sigma(h^{-1} = \infty, 1, \epsilon) \sim |\epsilon|^{-s} \quad (4.5a)$$

and

$$\Sigma(h^{-1}, 1, \epsilon=0) \sim h^{-1+u}. \quad (4.5b)$$

Since by Sec. III A, we have

$$\Sigma(h^{-1}, 1, \epsilon) = h^{-1} \Sigma(1, h, \epsilon)$$

so that if  $\Sigma(1, h, \epsilon=0) \sim h^u$  as  $h \rightarrow 0$ , then  $\Sigma(h^{-1}, 1, \epsilon=0) \sim h^{-1+u}$ . Therefore, the scaling form (4.3b) is unchanged except that the leading power  $h^u$  becomes  $h^{-1+u}$ , and the crossover exponent is given by

$$\phi = (1 - u)/s. \quad (4.6)$$

Since the expressions for  $\phi$  in (4.4) and (4.6) must be identical, we can eliminate the "critical isotherm" exponent  $u$  to obtain an expression for  $\phi$  in terms of the "thermal-like" exponents of the pure RRN and RSN limits,

$$\phi = 1/(\mu + s). \quad (4.7)$$

Note that for  $d=2$ ,  $u = \frac{1}{2}$  by duality.<sup>25</sup> Hence from (4.4) and (4.6) we have

$$\mu = s \quad (d=2). \quad (4.8)$$

Moreover, for  $d=2$  we can show that more generally

$$g(-x) = 1/g(x), \quad (4.9)$$

where  $g(0)=1$  by definition. Therefore, if the scaling function is known for  $p > p_c$ , we obtain it for  $p < p_c$  simply by (4.9). In Ref. 5 we have shown by using Monte Carlo simulations that the scaling *ansatz* (4.3b) is justified and  $g(x)$  satisfies relation (4.9). A rigorous proof of (4.9) is given in Appendix A.

## V. SCALING FOR THE rms DISPLACEMENT FOR THE RRN AND RSN LIMITS

Already with  $h=0$ , the scaling of  $R(t)$  is subtle and the results are quite rich. Hence, we devote this section to the  $h=0$  case, deferring to Sec. VI the general- $h$  discussion.

### A. Scaling of $R(1, 0, \epsilon, t)$ for the RRN limit

Many of the results of the RRN limit have been already proposed.<sup>8-11</sup> Here we present a particularly simple derivation of the scaling behavior; we will later generalize our RRN result to the RSN limit, and to the general two-component system as well.

The physics of the RRN is completely different below and above  $p_c$ . Below  $p_c$  the walker (de Gennes ant) is trapped inside the finite cluster. Hence,

$$\lim_{t \rightarrow \infty} R^2(1, 0, \epsilon, t) = R_s^2(\epsilon) \sim |\epsilon|^{-2\nu+\beta} \quad (p < p_c), \quad (5.1a)$$

where  $R_s(\epsilon)$  is the mean radius of a finite cluster, and  $\epsilon = (p_c - p)/p_c$  as above (see Fig. 7).

Above  $p_c$ , there is a tenuous infinite network so the mean-square displacement (averaged over all configura-

tions) is not bounded by  $R_s^2$ . We expect from the Nernst-Einstein relation that  $R^2/t \sim D \sim |\epsilon|^\mu$ , so

$$R^2(1, 0, \epsilon, t) \sim t |\epsilon|^\mu. \quad (5.1b)$$

Accordingly, one is led to a general scaling *ansatz*

$$R^2(1, 0, \epsilon, t) \sim t |\epsilon|^\mu A_\pm(t/|\epsilon|^{-z}), \quad (5.2)$$

where  $A_-(x)$  denotes the ant scaling function below  $p_c$  and  $A_+(x)$  is the corresponding scaling function above  $p_c$ .

Now  $A_\pm(x)$  must have the following properties: (a) In order that (5.1a) be satisfied,  $R^2(t) \rightarrow R_s^2$  for  $p < p_c$  and  $t \gg |\epsilon|^{-z}$ . Hence,

$$A_-(x) \sim 1/x \quad (x \gg 1). \quad (5.3a)$$

(b) In order that (5.1b) be satisfied,

$$A_+(x) = \text{const.} \quad (x \gg 1). \quad (5.3b)$$

Note that the crossover exponent  $z$  in (5.2) is readily determined by substituting (5.3a) into (5.2) and comparing with (5.1a),

$$z = \mu + 2\nu - \beta. \quad (5.4)$$

For length scales much less than the correlation length, the substrate cluster is self-similar. Hence, a random walker on this substrate cannot distinguish the fact that the system is not at the critical point—i.e.,  $p \neq p_c$ . Hence, for times less than a "crossover time"  $t_1 = |\epsilon|^{-z}$  the walk statistics have the same scaling properties as those exactly at  $p_c$ . For this reason, we expect  $R^2(1, 0, \epsilon, t)$  to be independent of  $\epsilon$  for  $t < t_1$ . By definition,

$$R^2(1, 0, \epsilon, t) \sim t^{2k} \quad (t < t_1). \quad (5.5)$$

In order that (5.5) be satisfied, we require that

$$A_\pm(x) \sim x^{2k-1} \quad (x \ll 1). \quad (5.6)$$

Hence,  $R^2$  in (5.2) will be independent of  $\epsilon$  only if  $k$  is related to the conventional critical exponents through

$$k = (2\nu - \beta)/[2(\mu + 2\nu - \beta)]. \quad (5.7)$$

Note that if the walker's starting point was constrained to the incipient infinite cluster, then  $2k$  would be replaced by  $2/d_w$ , where  $d_w = 2 + \mu/\nu - \beta/\nu$ . The anomalous diffusion law (5.5), valid for small times, reflects the fractal structure of the substrate on short length scales. As we approach  $p_c$ ,  $t_1 \rightarrow \infty$  and the regime of anomalous diffusion becomes arbitrarily large.

### B. Scaling of $R(\infty, 1, \epsilon, t)$ for the RSN limit

Here we focus entirely on  $p < p_c$ , and present a new scaling formulation for the RSN limit. For the RRN limit, the walker reaches  $R_s$  asymptotically, i.e.,  $R \rightarrow R_s$  as  $t \rightarrow \infty$ . However, for the RSN the walker (de Gennes termite) reaches the cluster radius already at infinitesimally small times, i.e.,

$$R \rightarrow R_s \quad (t \rightarrow 0^+). \quad (5.8a)$$

For large times, it follows from the Nernst-Einstein relation that

$$R^2 \sim t |\epsilon|^{-s} \quad (t \rightarrow \infty). \quad (5.8b)$$

Note that (5.8a) and (5.8b) for the RSN are analogous to (5.1a) and (5.1b) for the RRN. However, (5.8a) and (5.8b) both concern  $p < p_c$  but two different time limits, while (5.1a) and (5.1b) both concern the same  $t \rightarrow \infty$  time limit but two different domains of  $p - p_c$ .

For the RRN problem, the  $p < p_c$  and  $p > p_c$  regimes were bridged by the scaling *ansatz* (5.2). For the RSN problem,  $p < p_c$  but the short-time and long-time regimes of (5.8a) and (5.8b) can be bridged by the *ansatz*

$$R^2(\infty, 1, \epsilon, t) \sim t |\epsilon|^{-s} T_-(t/|\epsilon|^{-z'}) . \quad (5.9)$$

Now  $T_-(x)$  must have the following properties: (a) In order to satisfy (5.8a), we require

$$T_-(x) \sim 1/x \quad (x \rightarrow 0^+) . \quad (5.10a)$$

(b) In order to satisfy (5.8b), we must have

$$T_-(x) = \text{const.} \quad (x \gg 1) . \quad (5.10b)$$

The crossover exponent  $z'$  appearing in (5.9) may be found on substituting (5.10a) into (5.9) and comparing with (5.8a),

$$z' = -s + 2\nu - \beta . \quad (5.11)$$

Note that (5.11) has the same form as (5.4) except that the RRN exponent  $\mu$  is replaced by the RSN exponent  $-s$ .

### VI. SCALING OF THE rms DISPLACEMENT FOR GENERAL $h$

In the previous section we carried out a scaling analysis of the rms displacement  $R$  for the pure RRN (ant) and the pure RSN (termite) limits. In this section we will consider the general case where the fieldlike parameter  $h = \sigma_b/\sigma_a$  is not zero. Thus this section corresponds to a completely arbitrary two-component random material such as that described in the introduction (Fig. 1). First we consider the vicinity of the RRN limit, and later we will use Eq. (3.7) to transform to the vicinity of the RSN limit.

We begin by generalizing the  $h=0$  scaling *ansatz* of Eq. (5.2) and the  $t = \infty$  *Ansatz* for the long time diffusion constant of Eq. (4.3b) to

$$R^2(1, h, \epsilon, t) \sim t |\epsilon|^\mu G_\pm(t/|\epsilon|^{-z}, h/|\epsilon|^{1/\phi}) . \quad (6.1)$$

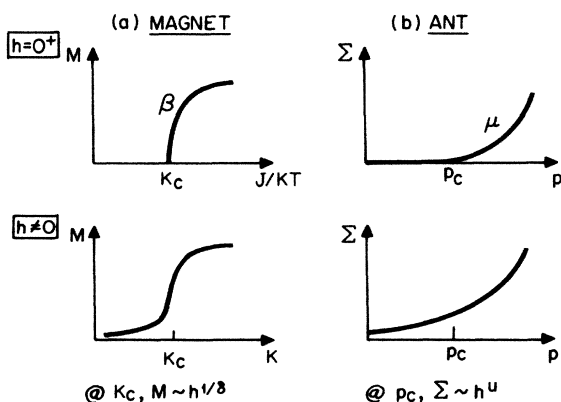


FIG. 5. Analogy between (a) a ferromagnet and (b) a random mixture.

Corresponding to the second variable  $h$  is a second crossover exponent  $\phi$ ; the two crossover exponents  $z$  and  $\phi$  are given by Eqs. (5.4) and (4.7). The subscript indicates, as above, the sign of  $p - p_c$ , and we shall consider mainly  $p$  below  $p_c$ .

For the magnetic system, there are two relevant scaling regions (Fig. 6). By analogy, we expect there to be two scaling regions for the present problem, which we denote as region  $\alpha$  ( $h \ll |\epsilon|^{1/\phi}$ ) and region  $\beta$  ( $1 \gg h \gg |\epsilon|^{1/\phi}$ ) (see Fig. 6).

#### A. Scaling for region $\alpha$ ( $h \ll |\epsilon|^{1/\phi}$ ) close to the RRN limit

Since  $h/|\epsilon|^{1/\phi}$  is small, we have

$$R^2(1, h, \epsilon, t) = t |\epsilon|^\mu [G_-(t/|\epsilon|^{-z}, 0) + h/|\epsilon|^{1/\phi} G_1(y^\delta t/|\epsilon|^{-z})] , \quad (6.2)$$

where the second term is the leading contribution to the small values of  $h$  and  $y = h/|\epsilon|^{1/\phi}$ . Note that the second term in (6.2) vanishes as  $h \rightarrow 0$ , so that we recover the RRN scaling relation (5.2).

In (6.2) we have assumed that the  $t$  and  $h$  dependence of  $G_1$  enters only in the product form  $th$ . We can further argue that  $\delta=1$ . To see this, recall the general relation (3.7) that  $R^2$  of a system near the RRN limit is identical, if  $t$  is replaced by  $t/h$ , to  $R^2$  for a system near the RSN limit. Thus if we perform the transformation  $t \rightarrow t/h$ , (6.2) becomes

$$R(1, h, \epsilon, t/h) = R(h^{-1}, 1, \epsilon, t) ,$$

i.e.,

$$R^2 = (t |\epsilon|^\mu / h) G_-(t/h |\epsilon|^{-z}, 0) + t |\epsilon|^{\mu-1/\phi} G_1(th^{\delta-1} |\epsilon|^{-z-\delta/\phi}) . \quad (6.3)$$

For  $h \rightarrow 0$  we approach the RSN limit. Then for any nonzero  $t$  the first term tends as  $h \rightarrow 0$  to  $R_s^2$  (see Sec. V), while the second term also becomes independent of  $h$ , approaching  $t |\epsilon|^{-s}$  for large times (see Secs. III and V). Hence, we require from the argument of  $G_1$  in (6.3) that  $\delta=1$ . With  $\delta=1$ , we have from (6.1) and (6.2) that

$$R^2(1, h, \epsilon, t) \sim t |\epsilon|^\mu G_-(t/|\epsilon|^{-z}, 0) + th |\epsilon|^{-s} G_1(th/|\epsilon|^{-z'}) , \quad (6.4)$$

where we have used Eqs. (4.7) and (5.11). Comparison of (6.4) and (5.2) yields

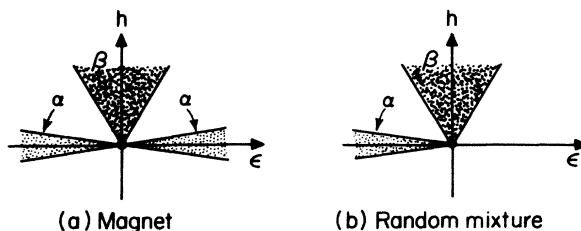


FIG. 6. Scaling regions  $\alpha$  and  $\beta$  for the simple ferromagnet and random mixture.

$$G_-(t/|\epsilon|^{-z}, 0) = A_-(t/|\epsilon|^{-z}). \quad (6.5)$$

In Eq. (6.4) we distinguish between three different time regimes [Fig. 8(a)], which are separated by two crossover times,

$$t_1 = |\epsilon|^{-z}, \quad (6.6a)$$

and

$$t_2 = |\epsilon|^{-z'}/h. \quad (6.6b)$$

First we give a rough physical interpretation of the two crossover times involved.

For  $t \ll t_1$  (regime I) the walker is just beginning to explore the bulk interior of whatever finite cluster he landed on. This is the self-similar region of the walk since the underlying substrate is self-similar for scales much smaller than  $t_1$ . This crossover time scales as  $R_s^{1/k}$ ,

$$R_s^{1/k} \sim |\epsilon|^{-z}, \quad (6.7)$$

where  $k$  and  $z$  are given by Eqs. (5.7) and (5.4).

For  $t_1 \ll t \ll t_2$  (regime II) the walker continually tries to escape completely from the cluster but he continually fails because most of the perimeter sites belong to the screened interior. In fact, the walker may temporarily leave the cluster but if he leaves in the screened region he will stumble again on the same cluster before breaking completely free. This is indicated schematically in Fig. 1 of Ref. 3. Hence,  $R^2$  does not increase, and we see a plateau.

Finally, for  $t \gg t_2$  (regime III), the walker completely escapes the cluster he started on by exiting from one of the unscreened "tiplike" portions of the cluster. Hence, there is an overall classical diffusion  $R^2 \sim Dt$ , with  $D$  extremely small. Specifically,  $D \sim h |\epsilon|^{-s}$  is related to the number of unscreened perimeter sites, since the exit frequency should scale as the ratio of unscreened perimeter sites  $M_u$  to the total number of all cluster sites  $M_{\text{tot}}$ ,<sup>3</sup> multiplied with the probability that the walker can step out from an unscreened site,

$$t_2^{-1} \sim (M_u/M_{\text{tot}})h. \quad (6.8a)$$

Here  $M_{\text{tot}}$  is the total number of cluster sites,

$$M_{\text{tot}} \sim \xi^{d_f}, \quad (6.8b)$$

and  $M_u$  is the number of unscreened perimeter sites

$$M_u \sim \xi^{d_u}. \quad (6.8c)$$

Relation (6.8c) defines the dimension  $d_u$  of the unscreened sites of a percolation cluster. From (6.8) we have

$$t_2^{-1} \sim h \xi^{d_u - d_f} \sim h |\epsilon|^{+z'}, \quad (6.9)$$

where  $z' = -s + 2\nu - \beta$  by Eq. (5.11). Hence,

$$d_u = d_f - (2\nu - \beta - s)/\nu, \quad (6.10)$$

which for  $d=2$  reduces to  $d_u = s/\nu$ . Next we consider quantitative predictions for each of the three time regimes. First, we define regime I as

$$t \ll t_1 = |\epsilon|^{-z} \ll t_2 = |\epsilon|^{-z'}/h \quad (\text{regime I}).$$

At very small times, we can neglect the second term in (6.4) and so recover the equation describing the short time behavior of the de Gennes ant,

$$R^2(1, h, \epsilon, t) \sim t^{1-\mu/z} \quad (\text{for regime I}), \quad (6.11a)$$

from Eq. (5.5). Second, we define

$$t_1 \ll t \ll t_2 \quad (\text{regime II}).$$

According to (5.1a), the first term becomes  $R_s^2$ , while the second term can be neglected. Therefore,

$$R^2(1, h, \epsilon, t) \sim |\epsilon|^{-2\nu+\beta} \quad (\text{for regime II}). \quad (6.11b)$$

Third, we define

$$t \gg t_2 \quad (\text{regime III}).$$

No matter how small  $h = \sigma_b/\sigma_a$  is, if we wait sufficiently long the walker will completely escape from the cluster and will walk on the low-conductivity regions of the network until it again encounters a cluster of high-conductivity bonds. For this reason, we intuitively expect the plateau in  $R^2(t)$  to give way to an increasing function. From the analogy with the RSN limit, we require  $G_1(x) = \text{const.}$  for  $x \gg 1$  [cf. Eq. (5.10b)], and, hence,

$$R^2(1, h, \epsilon, t) \sim |\epsilon|^{-2\nu+\beta} + th |\epsilon|^{-s} \quad (\text{regime III}). \quad (6.11c)$$

### B. Scaling for region $\beta$ ( $1 \gg h \gg \epsilon^{1/\phi}$ ) close to the RRN limit

In Sec. III we found that in the long-time limit for  $1 \gg h \gg \epsilon^{1/\phi}$ ,

$$R^2/t \sim D \sim \Sigma \sim h^u \quad (u = \phi\mu), \quad (6.12)$$

is independent of  $\epsilon$ . We therefore expect that also for finite times  $R^2$  should be independent of  $\epsilon$ . Therefore, (6.1) should reduce to the following scaling *ansatz* in region  $\beta$ :

$$R^2(1, h, \epsilon, t) \sim th^{\phi\mu} H[(t/|\epsilon|^{-z})(h/|\epsilon|^{1/\phi})^\alpha], \quad (6.13)$$

for both  $p > p_c$  and  $p < p_c$ . The exponent  $\alpha$  must be adjusted so that  $\epsilon$  does not appear in (6.6a). Hence,  $\alpha = \phi z$ , and (6.13) becomes

$$R^2(1, h, \epsilon, t) \sim th^{\phi\mu} H(th^{\phi z}). \quad (6.14)$$

To find the functional form of  $H(x)$ , we first note that for long times ( $t \gg t_h = h^{-\phi z}$ ), we require  $R^2 \sim th^{\phi\mu}$ . Hence,

$$H(x) \rightarrow \text{const} \quad (x \gg 1). \quad (6.15)$$

For  $t \ll t_h$  the motion of the walker is governed by the fractal structure of the substrate *alone*. Therefore, we expect that

$$R^2(1, h, \epsilon, t) \sim t^{2k} \quad (t \ll t_h) \quad (6.16)$$

is independent of  $h$ . Thus we have from (6.14)

$$H(x) \sim x^{-\mu/z} \quad (x \ll 1). \quad (6.17)$$

For  $h \rightarrow 0$ , the crossover time  $t_h$  tends to infinity and the anomalous diffusion (6.16) extends to all time scales.

### C. Scaling for region $\alpha$ close to the RSN limit

From (3.7) and (6.4) we obtain the mean-square displacement [see Fig. 8(b)] in the vicinity of the RSN limit

$$R^2(h^{-1}, 1, \epsilon, t) \sim t(|\epsilon|^\mu/h)G_-(t/h|\epsilon|^{-z}, 0) + t|\epsilon|^{-s}G_1(t/|\epsilon|^{-z'}). \quad (6.18a)$$

For  $t \gg h|\epsilon|^{-z}$ , the first term in (6.17) tends to  $R_s^2$ . Therefore, in order to reach the termite limit for times greater than 1,  $h \sim \sigma_b/\sigma_a$  has to satisfy the inequality

$$h \ll |\epsilon|^z, \quad (6.18b)$$

so that the first term of Eq. (6.17) approaches  $R_s^2 \sim |\epsilon|^{-2\nu+\beta}$  already at time of order 1. Hence, we only need consider the second term. To check the predictions of our scaling theory for the termite limit, we have undertaken extensive Monte Carlo computer simulations in a two-dimensional square lattice for times  $t \geq 1$  with a number of moves per unit on the  $A$  sites for  $h^{-1} \gg |\epsilon|^{-z}$ . We have determined  $R^2(h^{-1}, 1, \epsilon, t)$  for  $0.4 \leq p \leq 0.58$ . The result has been divided by  $|\epsilon|^{-2\nu+\beta}$  and plotted against  $t/|\epsilon|^{-z}$ , where  $-2\nu+\beta = -\frac{91}{36}$ , and  $z' = -\frac{91}{36} + 1.3 \simeq -1.2$  for  $d=2$  percolation. The result displayed in Fig. 9 confirms our scaling theory. Corresponding to the three time regimes—I, II, and III—near the RRN limit, near the RSN we have three time regimes: I', II', and III'. These are connected by the crossover times  $t'_1 = h|\epsilon|^{-z} = ht_1$  and  $t'_2 = |\epsilon|^{-z'} = ht_2$ . In regime I' ( $t \ll t'_1$ ), which shrinks to zero as  $h \rightarrow 0$ , the walk is governed by the fractal structure of the substrate. Therefore, we must have

$$R^2(h^{-1}, 1, \epsilon, t) \sim t^{1-\mu/z}, \quad (6.19)$$

which does not depend on  $\epsilon$ .

In regime II' ( $t'_1 \ll t \ll t'_2$ ) we have, in analogy to (6.11b),

$$R^2(h^{-1}, 1, \epsilon, t) \sim |\epsilon|^{-2\nu+\beta}. \quad (6.20)$$

In regime III' ( $t \gg t'_2$ ),

$$R^2(h^{-1}, 1, \epsilon, t) \sim |\epsilon|^{-2\nu+\beta} + t|\epsilon|^{-s}. \quad (6.21)$$

In contrast to the RRN limit, where the motion of the walker is governed by the interior bulk properties of the

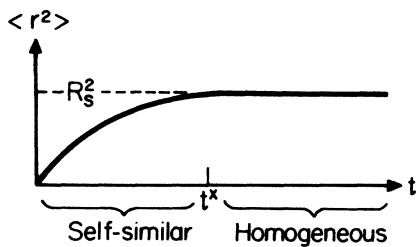


FIG. 7. Schematic dependence of mean-square displacement on time for a system slightly below  $p_c$ . For  $t < t_1$ , the walker samples a self-similar region smaller than the correlation length so the diffusion is anomalous ( $\langle r^2 \rangle \sim t^{2k}$ ). Above  $t_1$ , the walker saturates the finite clusters, whose average diameter scales as  $R_s$ , where  $R_s^2$  diverges as  $|\epsilon|^{-2\nu+\beta}$ .

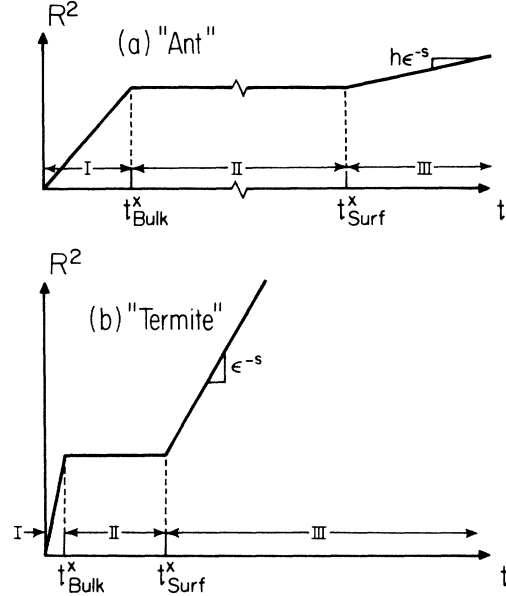


FIG. 8. (a) Dependence of the mean-square displacement time for a system near the random resistor network (RRN) or ant limit, and (b) a corresponding plot for the random superconductor network (RSN) or termite limit. As discussed in the text, there are now *two* crossover times,  $t_1$ , which depends on the "bulk" fractal properties, and  $t_2$ , which depends on the surface fractal properties.

finite clusters on a time scale  $t \sim |\epsilon|^{-z}$ , the motion of the walker close to the RSN limit is governed by the attempts of the walker to find *unscreened* sites of a high conducting cluster. Therefore, on a time scale  $t \sim |\epsilon|^{-z'}$ , the walker stays close to the surface of the finite cluster before leaving it. The time  $|\epsilon|^{-z'}$  is proportional to the ratio of the average number of unscreened and screened sites on a finite cluster. While close to the RRN limit the bulk properties of the finite clusters are probed, the surface properties of them are studied close to the RSN limit. In the termite limit already at infinitesimally short times the walker reaches the surface of a finite cluster. That is,  $R^2 \rightarrow R_s^2$ , where  $R_s^2$  depends strongly on  $\epsilon$ . There exists *no* finite time regime where  $R^2$  is independent of  $\epsilon$ . Therefore, a scaling *ansatz*  $R^2 \sim t^{2k'}$  analogous to (5.5), in connection with (5.9), cannot be made.<sup>3</sup> Indeed, such a scaling *ansatz* yields

$$1/k' = 2z'/(2\nu - \beta), \quad (6.22)$$

which makes the prediction  $k' \cong 1$  for  $d=2$ , and so predicts nearly ballistic behavior in two dimensions.

### D. Scaling for region $\beta$ close to the RSN limit

From (3.7) and (6.14) we obtain

$$R^2(h^{-1}, 1, \epsilon, t) \sim th^{\phi\mu-1}H(th^{\phi z-1}). \quad (6.23)$$

Following Sec. VI B, we distinguish between two time regimes with a crossover time

$$t'_h = ht_h = h^{-\phi z+1}. \quad (6.24)$$



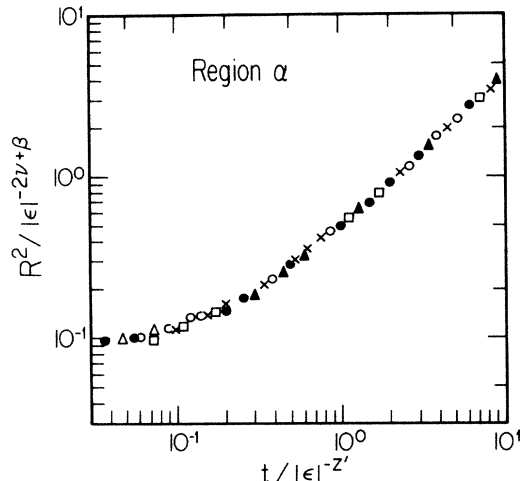


FIG. 9. Mean-square displacement multiplied by  $\epsilon^{2\nu-\beta}$  plotted against  $t|\epsilon|^{-2\nu-\beta}$  for values of  $h \gg |\epsilon|^{-(2\nu+\beta-s)}$ . Data are for several values of  $\epsilon$ , which here denotes  $p_c - p$ :  $p=0.55$  ( $\bullet$ ),  $p=0.54$  ( $\triangle$ ),  $p=0.53$  ( $\circ$ ),  $p=0.52$  ( $\square$ ),  $p=0.50$  ( $\times$ ), and  $p=0.45$  ( $\blacktriangle$ ). The data collapse confirms the validity of the scaling *ansatz* (6.4). For details of the Monte Carlo calculation see Ref. 5.

In two dimensions  $-\phi z + 1 \cong -\frac{1}{2}$ , and therefore the crossover time tends to infinity as  $h \rightarrow 0$ . For  $t \ll t_h'$ , we again expect anomalous diffusion  $R^2 \sim t^{2k}$ , while for  $t \gg t_h'$  we must have  $R^2 \sim t h^{\phi\mu-1}$ . We have checked our scaling *ansatz* (6.23) by performing Monte Carlo simulations at  $p=p_c$  for various values of  $h$  (see Fig. 10). The results led to a data collapsing as predicted by (6.23), which nicely confirms the validity of the present scaling approach.

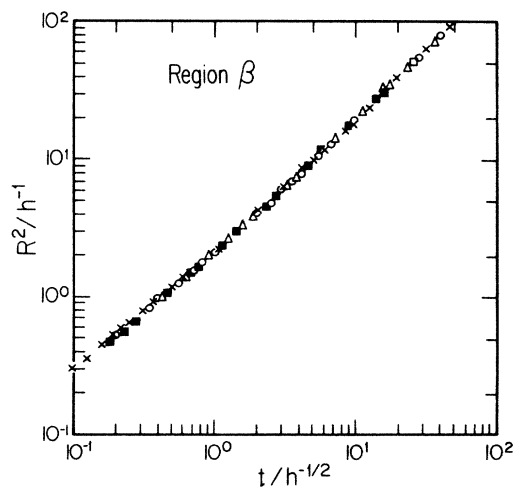


FIG. 10. Mean-square displacement times  $h$  vs  $th^{1/2}$  for  $p=p_c$  and several values of  $h$ :  $h=10^{-1}$  ( $\triangle$ ),  $h=5 \times 10^{-2}$  ( $\blacksquare$ ),  $h=10^{-2}$  ( $\circ$ ), and  $h=10^{-3}$  ( $\times$ ). The data collapse confirms the validity of the scaling *ansatz* (6.23). For details of the Monte Carlo calculation we refer to Ref. 5.

## VII. SUMMARY

In this work, we have discussed an exact transformation for the mean-square displacement of a random walker in a two-component random material. This exact transformation was used to develop a scaling theory for the mean-square displacement of the walker near the random superconducting limit (the "termite problem"). We predict three distinct time regimes, and these predictions are successfully confirmed by computer simulations. Since the long-time regime is related to the conductivity, the diffusion model discussed here provides also an efficient tool to calculate the conductivity exponents.

## ACKNOWLEDGMENTS

The authors wish to thank J. Adler, A. Aharony, S. Alexander, S. Havlin, F. Leyvraz, D. Stauffer, M. J. Stephen, and A. M. Tremblay for stimulating discussions and correspondence. This work was supported in part by a Consiglio Nazionale della Ricerca—National Science Foundation (CNR-NSF) exchange grant, by the Deutsche Forschungsgemeinschaft, and by grants to the Center for Polymer Studies by the Office of Naval Research, NSF, and the Army Research Office.

## APPENDIX A: EXACT RESULTS IN TWO DIMENSIONS

Equation (4.9),  $g(x) = 1/g(-x)$ , is the direct consequence of a duality argument valid in two-dimensional square-bond percolation. Note first that

$$g(x) = \Sigma(1, h, \epsilon) / \Sigma(1, h, 0), \quad (\text{A1})$$

with  $x = \epsilon/h^\phi$  and  $\epsilon = (p - p_c)/p_c$  with  $p_c = \frac{1}{2}$ . From the exact duality relation we have for the square lattice<sup>25,26</sup>

$$\Sigma(1, h, \epsilon) \Sigma(1, h, -\epsilon) = h, \quad (\text{A2})$$

which at  $p_c$  gives

$$\Sigma^2(a, h, 0) = h. \quad (\text{A3})$$

From (A1)–(A3) follows  $g(x) = 1/g(-x)$ .

## APPENDIX B: RELATION BETWEEN THE MODELS USED IN REFS. 3 AND 5

In this appendix we briefly explain the two models we have used to test our scaling predictions. In model I (Refs. 3 and 5) (see Sec. II), the walker's unit time per step  $f_i^{-1}$  is inversely proportional to the conductivity, i.e.,  $f_B/f_A = \sigma_B/\sigma_A$  [Eq. (2.1)] and the transition probability at a given site,  $\pi_i$ , to the  $i$ th nearest-neighbor sites is proportional to the conductivity, i.e.,  $\pi_i = f_i / \sum_j f_j$ , where the sum extends over the nearest neighbor of site  $i$ .

In model II,<sup>5</sup> the rules for the walker are slightly different. When the walker is on a  $B$  cluster, it chooses at random any direction and proceeds to this neighbor regardless of whether it is a  $B$  site or an  $A$  site. The corresponding step frequency is  $f_B = 1$ . When the walker is on an  $A$  site, it chooses at random in which direction its next attempt to move to a nearest-neighbor site will be (a) if

the attempted site belongs to an  $A$  cluster, the walker steps and the time not counted, or (b) if the attempted site belongs to a  $B$  cluster; then the walker can either step or wait, with probability  $\pi_{AB} \sim h$  and  $1 - \pi_{AB} \sim 1 - h$ , respectively.

The limit  $\pi_{AB} \rightarrow 1$  in model II corresponds to the limit  $h = f_B / f_A \rightarrow 0$  in model I. Both models are intimately related to each other in the following sense. Consider model I. By the detailed balance condition, the average time  $t_A$  the walker spends on  $A$  sites, and the average time  $t_B$  the walker spends on  $B$  sites are simply related by

$$t_A / t_B = p / (1 - p). \quad (\text{B1})$$

Let us now consider a variation of model I (which we call model I') for which time is not counted inside an  $A$  cluster. Then the corresponding diffusion constant in this model will be enhanced simply by a factor  $1/(1-p)$ . The difference between model I' and model II lies merely in the fact that in model I' the walker always has to jump, like "a myopic walker," while in model II the walker can wait like "a blind walker." It has been shown recently that both kinds of walker belong to the same universality class.<sup>27</sup> We verified, by extensive simulation of  $R^2(t)$ , that model I and model II also belong to the same universality class.

\*Present address: Institute for Theoretical Physics, University of California, Santa Barbara, CA 93106.

†Permanent address: Dipartimento di Fisica, Mostra D'Oltremare, Pad. 19, I-80125 Napoli, Italy.

<sup>1</sup>P. G. de Gennes, *Recherche* 7, 919 (1976).

<sup>2</sup>P. G. de Gennes, *J. Phys. (Paris) Colloq.* 41, C3 (1980); see also P. G. de Gennes, *Scaling Concepts in Polymer Physics* (Cornell University Press, Ithaca, 1979), p. 217f.

<sup>3</sup>A. Coniglio and H. E. Stanley, *Phys. Rev. Lett.* 52, 1068 (1984).

<sup>4</sup>J. Adler, A. Aharony, and D. Stauffer, *J. Phys. A* 18, L129 (1985).

<sup>5</sup>A. Bunde, A. Coniglio, D. C. Hong, and H. E. Stanley, *J. Phys. A* 18, L137 (1985).

<sup>6</sup>B. G. Orr, H. M. Jaeger, and A. M. Goldman, *Bull. Am. Phys. Soc.* 30, 232 (1985).

<sup>7</sup>For a recent review of the experimental situation, see G. Deutscher, A. Kapitulnik, and M. Rappaport, *Ann. Israel Phys. Soc.* 5, 207 (1983).

<sup>8</sup>J. Straley, *J. Phys. C* 13, 2991 (1980).

<sup>9</sup>S. Alexander and R. Orbach, *J. Phys. (Paris) Lett.* 43, L625 (1982).

<sup>10</sup>D. Ben-Avraham and S. Havlin, *J. Phys. A* 15, L691 (1982).

<sup>11</sup>Y. Gefen, A. Aharony, and S. Alexander, *Phys. Rev. Lett.* 50, 77 (1983).

<sup>12</sup>R. Rammal and G. Toulouse, *J. Phys. (Paris) Lett.* 44, 43 (1983).

<sup>13</sup>H. Scher and M. Lax, *Phys. Rev. B* 10, 4491 (1974).

<sup>14</sup>A. Bunde, W. Dieterich, and E. Roman, *Phys. Rev. Lett.* 55, 5 (1985).

<sup>15</sup>A. Kapitulnik and G. Deutscher, *Phys. Rev. Lett.* 49, 1444 (1982).

<sup>16</sup>R. Voss, R. B. Laibowitz, and E. I. Alessandrini, *Phys. Rev. Lett.* 49, 1441 (1982).

<sup>17</sup>R. B. Laibowitz and Y. Gefen, *Phys. Rev. Lett.* 53, 380 (1984).

<sup>18</sup>B. J. Last and D. J. Thouless, *Phys. Rev. Lett.* 27, 1719 (1971).

<sup>19</sup>B. P. Watson and P. L. Leath, *Phys. Rev. B* 9, 4893 (1974).

<sup>20</sup>G. Deutscher, *J. Phys. C* 12, L219 (1979).

<sup>21</sup>J. G. Zabolitzky, *Phys. Rev. B* 30, 4077 (1984); H. J. Herrmann, B. Derrida, and J. Vannimenus, *ibid.* 30, 4080 (1984); D. C. Hong, S. Havlin, H. J. Herrmann, and H. E. Stanley, *ibid.* 30, 4083 (1984); C. J. Lobb and D. J. Frank, *ibid.* 30, 4089 (1984); J. W. Essam and F. M. Bhatti, *J. Phys. A* 18, 3577 (1985); A. Bunde, E. Roman, and W. Dieterich, *Solid State Ionics* (to be published).

<sup>22</sup>A. L. Efros and B. I. Shklovskii, *Phys. Status Solidi* 76, 475 (1976).

<sup>23</sup>D. Wilkinson, J. S. Langer, and P. N. Sen, *Phys. Rev. B* 28, 1081 (1983).

<sup>24</sup>More precisely,  $n$  is the ratio of the volume of the substrate to the total embedding volume. For example, if an ant walks only on the incipient infinite percolation cluster, then  $n$  scales with  $L$  as  $L^{d_f} / L^d = L^{-\beta/\nu}$ , where  $d_f$  is the fractal dimension. On the other hand, a termite can walk anywhere.

<sup>25</sup>J. Straley, *Phys. Rev. B* 15, 5733 (1977); *J. Phys. C* 9, 783 (1976); see also the recent review by B. G. Deutscher, R. Zallen, and J. Adler, in *Percolation Processes and Structures* (Hilger, Bristol, 1983).

<sup>26</sup>J. Bernasconi, W. R. Schneider, and H. J. Wiesman, *Phys. Rev. B* 15, 5250 (1977).

<sup>27</sup>I. Majid, D. Ben-Avraham, S. Havlin, and H. E. Stanley, *Phys. Rev. B* 30, 1626 (1984).